Lawrence Berkeley National Laboratory
Recent Work

Title
ELECTROCHEMISTRY OF THE SULFIDE/POLYSULFIDE COUPLE

Permalink
https://escholarship.org/uc/item/0fc1x6pz

Authors
Remick, R.J.
Camara, E.H.

Publication Date
1983-07-01

eScholarship.org Powered by the California Digital Library
University of California

LBL-16850
UC-94c

Lawrence Berkeley Laboratory

UNIVERSITY OF CALIFORNIA

RECEIVED
LAWRENCE
BERKELEY LABORATORY
JAN 17 1984
LIBRARY AND
DOCUMENTS SECTION

APPLIED SCIENCE DIVISION

ELECTROCHEMISTRY OF THE SULFIDE/POLYSULFIDE COUPLE

R.J. Remick and E.H. Camara

July 1983

TWO-WEEK LOAN COPY

This is a Library Circulating Copy which may be borrowed for two weeks. For a personal retention copy, call Tech. Info. Division, Ext. 6782.

APPLIED SCIENCE DIVISION

LBL-16850

Prepared for the U.S. Department of Energy under Contract DE-AC03-76SF00098

DISCLAIMER

This document was prepared as an account of work sponsored by the United States Government. While this document is believed to contain correct information, neither the United States Government nor any agency thereof, nor the Regents of the University of California, nor any of their employees, makes any warranty, express or implied, or assumes any legal responsibility for the accuracy, completeness, or usefulness of any information, apparatus, product, or process disclosed, or represents that its use would not infringe privately owned rights. Reference herein to any specific commercial product, process, or service by its trade name, trademark, manufacturer, or otherwise, does not necessarily constitute or imply its endorsement, recommendation, or favoring by the United States Government or any agency thereof, or the Regents of the University of California. The views and opinions of authors expressed herein do not necessarily state or reflect those of the United States Government or any agency thereof or the Regents of the University of California.

LBL-16850

ELECTROCHEMISTRY OF THE SULFIDE/POLYSULFIDE COUPLE

Project 65911 Final Report

for the Period November 1, 1982, to June 30, 1983

Robert J. Remick
Elias H. Camara

Prepared by
Institute of Gas Technology
IIT Center, 3424 S. State Street
Chicago, Illinois 60616

for

Lawrence Berkeley Laboratory
University of California
Berkeley, California 94720

Date Published — July 1983

This work was supported by the
Assistant Secretary for Conservation and Renewable Energy,
Office of Energy Systems Research, Energy Storage Division,
U.S. Department of Energy, under Contract No. DE-AC03-76SF00098,
Subcontract No. 4519690 with the Lawrence Berkeley Laboratory.

SUMMARY

The redox behavior of solutions containing sodium sulfide and sodium polysulfide was investigated using a platinum wire electrode. We determined that contrary to published literature, the equilibrium potential of the sulfide/polysulfide redox couple does have a pH-sensitive component. Experimental results indicate that platinum is not a good electrocatalyst for this couple, but that upon anodization a layer is formed on the surface of the platinum that imparts a reasonable catalytic activity to the electrode. A mechanism is proposed based on present results and past literature that accounts for most if not all of the observed phenomenon.

This proposed mechanism predicts that electronically conducting materials that contain sulfur as part of their chemical composition, specifically CoS, NiS, CuS, PbS, and MoS_2, should be excellent electrocatalysts for both anodic and cathodic reactions. This is confirmed for CoS, CuS, and PbS by the published work of Hodes et al.[4] This present work extends the range of materials investigated to include NiS and MoS_2 and two alternative methods for preparing sulfided electrodes. Experimental results indicate that MoS_2 is the preferred electyrocatalyst for the sulfide/polysulfide redox couple and that a relatively inexpensive composite electrode can be fabricated using 10% MoS_2, 80% carbon black, and 10% Teflon 30.

TABLE OF CONTENTS

	Page
INTRODUCTION	1
EXPERIMENTAL PROCEDURE	3
Chemicals	3
Solutions	3
pH Determination	3
Potentiometric Measurements	4
Ultraviolet-Visible Spectroscopy	4
Cyclic Voltammetry	4
Steady-State Tafel Plots	5
Micropolarization Measurements	6
RESULTS AND DISCUSSION OF TASK 1	7
Redox Potential as a Function of pH	7
Optical Spectra of Polysulfides	10
Steady-State Measurements	12
Cyclic Voltammetry	20
RESULTS AND DISCUSSION OF TASK 2	25
Assessment of Electrocatalytic Activity	25
Nickel Sulfide	26
Cobalt Sulfide	28
Molybdenum Sulfide	29
Concentration Effects on Electrode Performance	31
Composite Electrodes	32
CONCLUSIONS	35
REFERENCES CITED	37

LIST OF FIGURES

Figure No.		Page
1	Relationship Between Changes in pH and Changes in Electrode Potential for Sulfide/Polysulfide in 1M Sodium Chloride	8
2	Typical Ultraviolet Absorption Spectra for Solutions at 10-to-1 Dilution	11
3	Tafel Plots for Anodic Reaction in 1M Sodium Hydroxide	14
4	Linear Plot of Current Density Versus Overpotential for Cathodic Reaction in 1M Sodium Hydroxide	16
5	Linear Plot of Current Density Versus Overpotential for Cathodic Reaction in 1M Sodium Chloride	17
6	Cyclic Voltammogram of the 20th Cycle Using a 0.85 cm^2 Platinum Wire Electrode in Solution No. 2	21
7	Cyclic Voltammogram for the First, Second, and Third Cycles Using a Platinum Wire in Solution No. 2	23
8	Cyclic Voltammogram of Nickel Sulfide in Solution No. 13	27
9	Cyclic Voltammogram of Cobalt Sulfide in Solution No. 13	28
10	Cyclic Voltammogram of Molybdenum Wire in Solution No. 13	30
11	Cyclic Voltammogram of Molybdenum Wire With Molybdenum Coating in Solution No. 13	31
12	Performance of MoS_2 Wire Electrode in Solutions of Varying Concentration	33
13	Performance of Composite Electrode in Solution No. 130	34

LIST OF TABLES

Table No.		Page
1	Potential and pH Data by Solution Number	7
2	Acid Dissociation Constants for Sulfanes	9
3	Spectral Characteristics of Polysulfide Ions	11
4	Calculated Absorbance of Solution Nos. 3 and 13	13
5	Optical Absorption of Solutions at 370 nm	13
6	Steady-State Data for Anodic Reaction	15
7	Steady-State Data for Cathodic Reaction	18
8	Equilibrium Potential and Exchange Density for Various Metals and Their Sulfide in Solution No. 13	26
9	Parameters Investigated and Results Obtained for the Polarization of MoS_2 Wire Electrodes in Solutions of Varying Concentration	33

INTRODUCTION

The fact that alkali metal sulfides and sulfur form a reversible redox couple in aqueous solution has been known for some time.[1] But interest in this redox couple has been renewed because of the recent discovery that cadmium chalcogenide photoelectrodes can be stabilized by the addition of sulfide ions to aqueous solutions in contact with the electrode surface.[5,9] Recently, several articles[4,5] have proposed the sulfide/polysulfide couple as an active material for an aqueous electrochemical storage device capable of photoelectrochemical recharge. Recent investigations at the Institute of Gas Technology (IGT), however, have shown discrepancies between the assumed behavior based upon the scientific literature and actual experimental results for aqueous sulfide/polysulfide solutions.

The most definitive study to date of the electrochemistry of the sulfide/polysulfide couple is a paper by Allen and Hickling[1] published in 1957. This paper gives the following formula for calculating the reversible electrode potential of an inert electrode in an aqueous solution that contains sodium hydroxide, sodium sulfide, and dissolved sulfur. The formula is applicable over a wide range of sulfur and sulfide concentrations:

$$E = -0.522 + 0.033 \log [S] - 0.058 \log [Na_2S] \qquad (1)$$

However, if this formula were used to predict the potential of an inert electrode in a similar solution of equivalent sulfide/sulfur concentration, but made up using sodium chloride as a supporting electrolyte, the calculated values fall from 60 to 100 mV negative of the experimentally determined values. Allen and Hickling also reported that upon anodic polarization the current flow followed a Tafel law consistent with an electron transfer rate limitation. Furthermore, when an electrode was placed on open circuit after being polarized anodically, it quickly returned to a reproducible potential close to the calculated value. Ives[6] interpreted Allen and Hickling's results as indicating that the only processes involved are as follows:

$$S + S^{2-} \rightarrow S_2^{2-} \qquad (2)$$

$$S_2^{2-} + 2e^- \rightleftarrows 2S^{2-} \qquad (3)$$

Experiments at IGT using platinum electrodes confirmed Allen and Hickling's results for anodic polarizations. But when polarized cathodically, a Tafel plot with a different slope was obtained, and excessive periods of time

were required to reestablish the open-circuit potential. Furthermore, under some conditions the current density at 100 mV cathodic overpotential was nearly an order of magnitude lower than that obtained at 100 mV anodic overpotential in solutions containing equal molar sulfur and sulfide.

This program was divided into two tasks. The purpose of Task 1 was to investigate the various reaction mechanisms associated with the sulfide/polysufide redox couple on platinum. The purpose of Task 2 was to use this information to identify more promising electrocatalytic materials that exhibit rapid electrode kinetics, long lifetimes, and reasonable costs.

EXPERIMENTAL PROCEDURE

Chemicals

All chemicals used in the course of this work were reagent-grade materials from Fisher Scientific and were used as received without further purification. All solutions were prepared using deaerated-deionized water (>1 megaohm) and were mixed and stored under a nitrogen atmosphere. Cobalt wire electrodes were obtained from Goodfellow Metals and were over 99.99% pure. Platinum wire electrodes were obtained from Matthey Bishop and were over 99.9% pure. Nickel and molybdenum electrodes were obtained from Alfa Products and were 99.9% pure.

Solutions

Sulfide solutions (0.1M) were prepared by dissolving sodium sulfide nonahydrate ($Na_2S \cdot 9H_2O$) in 1.0N NaOH (Solution No. 1) and 1.0N NaCl (Solution No. 11) under nitrogen. Ultraviolet spectroscopy was used to verify that these solutions contained no polysulfides to the limit of detection (100 ppm sulfur at 370 nm).

Polysulfide solutions were prepared by first dissolving a quantity of sodium sulfide nonahydrate in the appropriate electrolyte and then adding measured amounts of sublimed sulfur. Three polysulfide solutions were prepared in 1N sodium hydroxide using sulfide-to-sulfur ratios of 2:1 (Solution No. 2), 1:1 (Solution No. 3), and 1:2 (Solution No. 4). A constant total sulfur content (sulfide + sulfur) was maintained at 0.1 mol/L. We also prepared three polysulfide solutions in 1N sodium chloride at sulfide-to-sulfur ratios of 2:1 (Solution No. 12), 1:1 (Solution No. 13), and 1:2 (Solution No. 14).

Two additional polysulfide solutions were prepared for Task 2 work. Solution No. 130 was formulated as 0.5M sodium sulfide, 0.5M sulfur, and 1.0M sodium chloride. Solution No. 1302 was formulated as 1.0M sodium sulfide and 1.0M sulfur with no supporting electrolyte.

pH Determination

The pH was calculated for Solution Nos. 1 through 4 on the basis of the sodium hydroxide added and by assuming complete hydrolysis of sodium sulfide to form bisulfide and hydroxide. For Solutions Nos. 11 through 24, which were

prepared using sodium chloride as the supporting electrolyte, pH was measured with a Corning Model 476223 Semi Micro Combined Electrode and a Markson Scientific Model 90 digital pH Meter. Measurements were reproducible to within ±0.05 pH unit, but were assumed to have an additional error of ±0.1 pH unit at pH 13 because of sodium ion interference at high ionic strength.

Potentiometric Measurements

The potential of the working electrode was measured against the reference electrode using a PAR Model 173 Potentiostat equipped with a PAR Model 178 Electrometer. A Fisher Model 130-639-52 Saturated Calomel Reference Electrode was used in all experimental measurements. Potential was measured under a nitrogen atmosphere with a nitrogen purge and rapid stirring.

Ultraviolet-Visible Spectroscopy

UV-Visible spectroscopic examinations were performed with a Perkin Elmer Model 200 UV-Visible spectrophotometer. Absorbtion spectra were taken of Solutions Nos. 1 and 11, which contained 0.1M sodium sulfide in 1.0M sodium hydroxide and 1.0M sodium chloride, respectively, using undiluted aliquots of the solutions. The purpose of this investigation was to determine the presence of polysulfide contaminants in the sulfide solution. Experiments with known samples indicated that polysulfide levels as low as 100 ppm were detectable in undiluted samples. Spectra of solutions containing millimolar quantities of polysulfide required a dilution of 10 to 1 to keep the absorbance below 1.0 at the 370 nm peak. Dilutions of 100 to 1 were required to keep the peak at 300 nm below an absorbance of 1.0 with those solutions containing high ratios of polysulfide to sulfide. Deionized water (>1 megaohm) was used for all dilutions.

Cyclic Voltammetry

Cyclic voltammetric investigations were performed using an H-cell of conventional design. The cell was fitted with a Nafion-125 separator between chambers. Each chamber held 250 mL of solution. Working electrodes were constructed from 1-mm-diameter wire mounted at one end in a Teflon block and held in a vertical position. Geometrical surface area exposed to solution was generally less than 1 cm^2. This combination of small electrode surface area and large solution volume allowed lengthy experimentation without appreciable changes in the concentrations of the active species in solution.

Cyclic voltammograms were recorded using a PAR Model 173 Potentiostat, a PAR Model 178 Electrometer, and a PAR Model 176 Current Follower driving a Hewlett Packard Model 7035B, X-Y recorder. A conventional triangular-wave generator was used to provide a sweep rate to the PAR of 100 mV/s. All voltammograms were taken under a nitrogen atmosphere in a quiet, unstirred solution. The reference electrode was in every case the Fisher saturated calomel electrode (SCE) mentioned above. A 50-cm^2 platinum wire gauge was used as a counter electrode. In experiments with Solutions Nos. 1 through 4, which contained 1.0M NaOH, the counter electrode compartment was filled with 1.0M sodium hydroxide plus 0.10M sodium sulfate. Sodium sulfate was used in place of sodium sulfide in the counter electrode compartment to prevent the build-up of sulfur deposits on the platinum counter electrode during potential sweeping and potential pulsing of the working electrode and to maintain an equal ionic strength on opposite sides of the Nafion separator to prevent liquid transfer by osmosis. In experiments with Solution Nos. 11 through 24, the counter electrode compartment contained 1.0M sodium chloride and 0.10M sodium sulfate. In experiments with solution No. 130, the counter electrode compartment contained 1.0M sodium chloride saturated with sodium sulfate. In experiments with Solution No. 1302, the counter electrode compartment contained a saturated solution of sodium sulfate.

Steady-State Tafel Plots

Steady-state Tafel plots were constructed from information gathered in a steady-state, potentiostatic operating mode. Using the PAR Potentiostat with electrometer and current follower, a working electrode of wire was held at a potential versus the reference electrode that indicated zero current flow. In all cases this potential was identical to the potential measured on open circuit. A voltage was then applied to the working electrode to raise or lower its potential in steps of 10 mV versus the reference electrode. This was accomplished by manual adjustment of the potentiostat. A constant potential was maintained from 1 to 5 minutes to reach steady-state. The steady-state current was then recorded, and the electrode was stepped to the next higher or lower potential. All steady-state measurements of this type were performed under a nitrogen atmosphere with nitrogen sparging and rapid stirring.

Micropolarization Measurements

In several experiments a classical Tafel relationship was not exhibited either because of mass transfer limitations or because of electrode passivation. In these instances micropolarization experiments were conducted to determine exchange current density. Using the PAR Potentiostat with electrometer and current follower, the working electrode was held at a potential versus the reference electrode that indicated zero current flow. Then using a Wenking Model SMP 72 Scanning Potentiometer, the voltage applied to the working electrode was raised or lowered in steps of 1 mV at a rate of 1.5 steps per minute. A current-voltage plot was constructed automatically by feeding the outputs of the electrometer and current follower into the x and y axis of a Houston Instruments Omnigraphic 100 Recorder.

RESULTS AND DISCUSSION OF TASK 1

Redox Potential as a Function of pH

Results

Table 1 is a list of the solutions used in this task and shows 1) the solution number, 2) the sulfide-to-sulfur ratio, 3) the pH of the solution, 4) the open-circuit potential of a platinum wire in the solution versus SCE, and 5) the potential of a cobalt wire in the solution versus SCE. Note that all solutions in Table 1 have a total sulfur content (sulfide and sulfur) of 0.10M. Solution Nos. 2, 12, and 22, for example, all have the same sulfide-to-sulfur ratio and differ only in their pH and supporting electrolyte. It is obvious from Table 1 that the redox potential of the sulfide/polysulfide couple has a significant, pH-dependent component.

Experiments were conducted to determine the relationship between pH and electrode potential using Solution Nos. 12, 13, and 14. A single-chamber cell was constructed and fitted with a combination pH electrode, a platinum wire

Table 1. POTENTIAL AND pH DATA BY SOLUTION NUMBER

Solution No.	Sulfide/Sulfur Ratio*	pH	Pt vs. SCE, V	Co vs. SCE, V
1	1:0	14.04	−0.759	−0.764
2	2:1	14.03	−0.721	−0.726
3	1:1	14.01	−0.712	−0.710
4	1:2	14.01	−0.689	−0.684
11	1:0	13.0	−0.665	−0.670
12	2:1	12.8	−0.660	−0.673
13	1:1	12.5	−0.644	−0.651
14	1:2	12.4	−0.610	−0.607
21	1:0	9.0	−0.543	--
22	2:1	8.6	−0.523	--
23	1:1	8.4	−0.500	--
24	1:2	9.0	−0.516	--

* Total sulfur from all sources is 0.1M.

electrode, a reference electrode (SCE), a magnetic stir bar, and a nitrogen bubbler. Sulfide/polysulfide solution (200 mL) was placed in the chamber and sparged with nitrogen for 30 minutes. Small aliquots of 1M HCl were added to the solution, and changes in the pH and in the open-circuit electrode potential (Pt versus SCE) were determined. The addition of acid to the solution produced a yellow precipitate in the portions of the solution where the local acid concentration was high. This precipitate was presumed to be sulfanes of formula H_2S_x ($x > 1$). As the solution was stirred, however, these precipitated sulfanes redissolved. Because this dissolution was slow, we allowed at least 5 minutes between acid additions in order to stabilize the solution pH. This process was continued until the precipitated sulfanes first failed to redissolve. The neutralized solutions thus produced from Solution Nos. 12, 13, and 14 were relabeled Solution Nos. 22, 23, and 24, respectively, and stored under nitrogen for later use.

As expected, the amount of acid required to reach the end point of the titration varied with the sulfide ion content of the solution: Solution No. 12 required 10.2 mL of 1M HCl, Solution No. 13 required 6.7 mL, and Solution No. 14 required only 3.2 mL. Figure 1 is a plot of the changes in electrode potential (ΔE) as a function of change in pH (ΔpH). Although each solution started with a pH and electrode potential characteristic of the

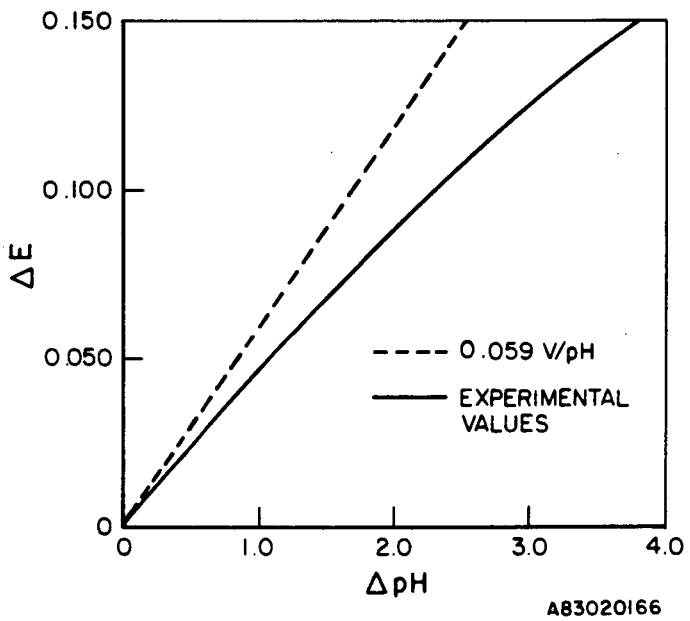


Figure 1. RELATIONSHIP BETWEEN CHANGES IN pH AND CHANGES IN ELECTRODE POTENTIAL FOR SULFIDE/POLYSULFIDE IN 1M SODIUM CHLORIDE

sulfide-to-sulfur ratio within that solution, a plot of ΔE versus ΔpH generated the same curve for all three solutions. Also, the rate of change, $\Delta E/\Delta pH$, for each solution measured after the addition of the first aliquot of acid yielded a rate of 0.059 V/pH. However, this rate of change decreased upon further acid additions to an average value of about 0.050 V/pH.

Discussion

Table 2 is a list of the first and second acid dissociation constants for the sulfane series from H_2S to H_2S_8. Table 2 shows that all the sulfanes from H_2S_2 to H_2S_8 will be completely dissociated in solutions with a pH above 11. Only the first member of the series H_2S will retain a single hydrogen in the pH of interest, pH 11 to pH 15. It is important to note that at the time of the original Allen and Hickling paper (1957) the second dissociation constant for hydrogen sulfide was generally accepted as 14. But in 1971 Giggenbach[2] measured the second dissociation constant (pk_2) at 17.1. Thus, Equation 3 is not the correct half-cell equation for the sulfide/disulfide redox couple, but rather Equation 4 is more correct:

$$S_2^{2-} + 2e^- \rightleftarrows 2S^{2-} \quad (3)$$

$$S_2^{2-} + 2H_2O + 2e^- \rightleftarrows 2HS^- + 2OH^- \quad (4)$$

Equation 4 predicts a pH dependence of 0.059 V/pH for the redox potential of the sulfide/polysulfide couple.

Table 2. ACID DISSOCIATION CONSTANTS* FOR SULFANES

Sulfane	pk_1	pk_2
H_2S	6.9	17.1
H_2S_2	5.0	9.7
H_2S_3	4.2	7.5
H_2S_4	3.8	6.3
H_2S_5	3.5	5.7
H_2S_6	3.2	5.2
H_2S_7	3.0	4.8
H_2S_8	2.9	4.4

* From Sulfur, Energy, and Environment.[7]

The experimental results reported above show that this is correct, but only for small changes in pH. At larger changes in pH, the pH dependence of the redox potential falls below 0.059 V/pH. (See Figure 1.) This can be explained in part by the second acid dissociation of disulfide. As a pH of 11 is approached, the protonated disulfide HS_2^- would have some stability; at a pH of 9.7, fully half of the disulfide present would be protonated. Thus at a pH of 9.7, Equations 4 and 5 would proceed in parallel:

$$HS_2^- + H_2O + 2e^- \rightleftarrows 2HS^- + OH^- \qquad (5)$$

Although Equation 4 predicts a redox potential with a pH dependence of 0.059 V/pH, Equation 5 predicts a dependence of only 0.0296 V/pH. Thus in the acid titration experiment above, the pH dependence of the redox potential is not expected to be constant from pH 12.9 to pH 8.4, but rather to deviate as in Figure 1.

It is beyond scope of this project to devise a formula for predicting the redox potential for the sulfide/polysulfide couple that accounts for all complex variables. Nevertheless, researchers attempting to predict the theoretical voltage of a redox device that utilizes aqueous sulfide/polysulfide as an active component may find that measured voltages deviate markedly from those predicted by the Allen and Hickling — especially when the pH of the solution deviates markedly from 14. Therefore, we have prepared Equation 6 to predict the redox potential of the sulfide/polysulfide couple by empirical fit with the data in Table 1:

$$E = -0.504 + 0.0296 \log [S^o] - 0.0592 \log [S^=] - 0.050 \log [OH^-] \qquad (6)$$

This equation appears to hold for dilute solutions of pH 11 to pH 14, but it should be expected to fail at high sulfur-to-sulfide ratios.[1,4]

Optical Spectra of Polysulfides

Giggenbach[3] investigated the optical absorption spectra of aqueous polysulfides from pH 6.8 to pH 17.5 at 20°C. Table 3 is a list of the polysulfides through pentasulfide, the wavelength of the maximum absorption (λmax) for the major peaks in the ultraviolet spectrum, and the molar absorptivity at λmax as reported by Giggenbach.[3] Table 3 shows that most of the polysulfides have strong absorptions at about 370 and 300 nm. Therefore, a mixture of polysulfides would be expected to exhibit an ultraviolet spectrum with two broad bands located near 370 and 300 nm. These two bands are evident in the absorption spectra of Solution Nos. 2, 3, and 4 in Figure 2.

Table 3. SPECTRAL CHARACTERISTICS OF POLYSULFIDE IONS*

Polysulfide	λmax, nm	ε
S_2^{2-}	358	850
S_3^{2-}	416	95
	303	1140
S_4^{2-}	368	320
	303	1140
S_5^{2-}	374	640
	300	2000

* From Giggenbach.[3]

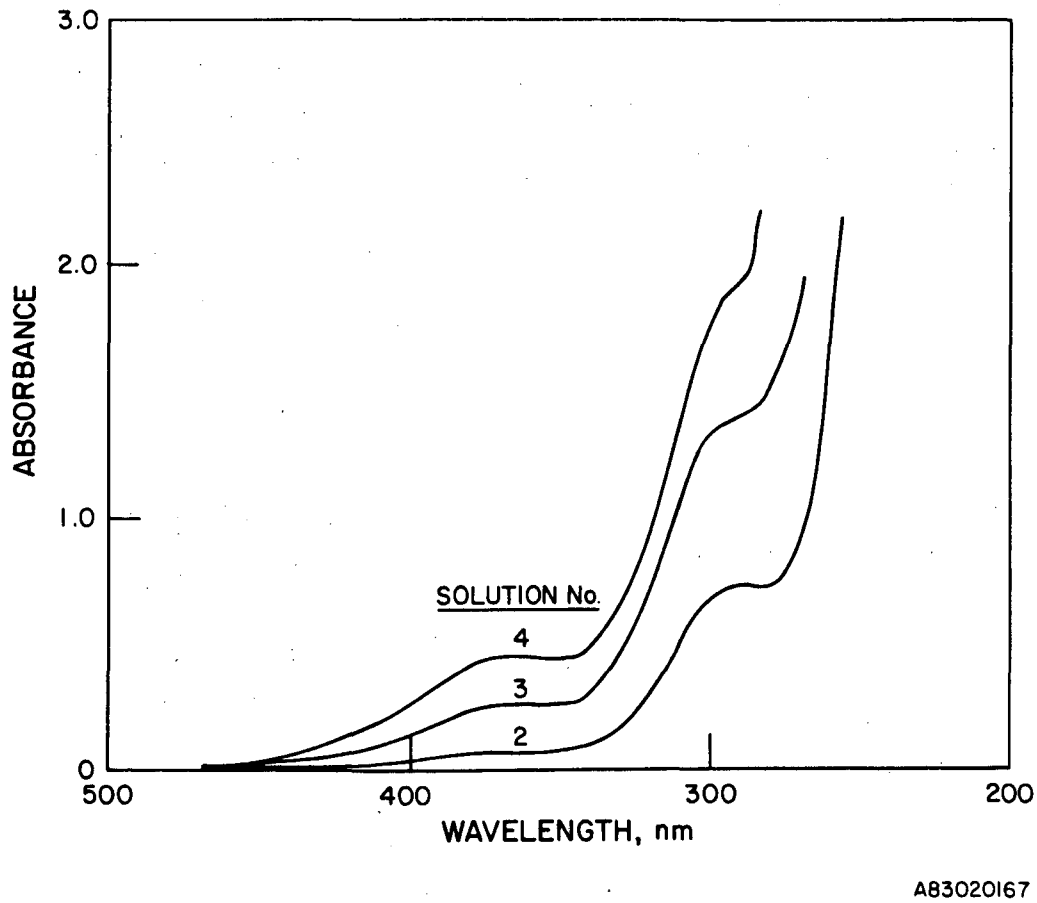


Figure 2. TYPICAL ULTRAVIOLET ABSORPTION SPECTRA FOR SOLUTIONS AT 10-TO-1 DILUTION

As indicated by the right hand column of Table 3, the total concentration of zero-valent sulfur in solution cannot be measured by a straightforward Beer's Law approach without knowing the concentrations of the various polysulfide ions. Giggenbach has gone to great lengths to formulate a method to determine the distribution of zero-valent sulfur among the various polysulfide species. Using the information provided by Giggenbach,[3] the concentration of the polysulfides can be calculated in, for example, Solution Nos. 3 and 13. Table 4 lists the various species, the calculated concentration of each species in Solution Nos. 3 and 13, the molar absorptivity for each species at 370 nm from Giggenbach,[3] and a calculated absorbance for each solution. Table 4 shows that although Solution Nos. 3 and 13 contain the same amount of zero-valent sulfur (0.050 mol/L), more sulfur is distributed among the higher polysulfides with high molar absorptivities for Solution No. 13 than for Solution No. 3. Table 4 predicts that Solution No. 13 should have 1.18 times greater absorbance than Solution No. 3. Table 5 lists the measured absorbances of Solution Nos. 1 through 14 and shows that Solution No. 13 does, in fact, have an absorbance 1.21 times greater than Solution No. 3, which is remarkably close to the ratio predicted. However, extreme caution should be used when comparing such data because the ionic strength of the solutions used by Giggenbach differ by an order of magnitude from those used here. Furthermore, Solution Nos. 11 through 14 contain a high concentration of chloride ion, which is not present in Solution Nos. 1 through 4 nor in any of Giggenbach's work.

Nevertheless, the data in Tables 4 and 5 illustrate the inadvisability of applying Beer's Law measurements to solutions of polysulfides. Furthermore, careful scrutiny of Giggenbach's work reveals that no isobestus points exist in the ultraviolet spectrum that are common to more than two polysulfide species at a time. Thus, ultraviolet spectroscopy cannot be applied to mixtures of polysulfides without detailed knowledge of additional solution parameters.

Steady-State Measurements

Results

Steady-state data for the anodic reaction appear to be well behaved for all solutions except No. 1. If we assume that the transfer coefficient (α) for the anodic reaction is 0.5 and that the number of electrons transferred

Table 4. CALCULATED ABSORBANCE OF SOLUTION NOS. 3 AND 13

Solution No. 3

Species	Concentration, M	ϵ_{370}	Absorbance
$S^{=}$	0.0314	0	--
$S_2^{=}$	0	--	--
$S_3^{=}$	0.0058	30	0.17
$S_4^{=}$	0.0128	300	3.84
$S_5^{=}$	0	--	--
		Total	4.01

Solution No. 13

Species	Concentration, M	ϵ_{370}	Absorbance
$S^{=}$	0.0329	0	--
$S_2^{=}$	0	--	--
$S_3^{=}$	0.0017	30	0.05
$S_4^{=}$	0.0151	300	4.53
$S_5^{=}$	0.0003	570	0.17
		Total	4.75

Table 5. OPTICAL ABSORPTION OF SOLUTIONS AT 370 nm

Solution No.	Dilution	Absorbance
1	none	0.0
2	10:1	0.078
3	10:1	0.299
4	10:1	0.46
11	none	0.0
12	10:1	0.100
13	10L1	0.361
14	10:1	0.94

per mole of reactant (n) is 2, then the steady-state data should indicate typical Tafel behavior at overpotentials above about 60 mV, barring mass transfer effects. A plot of log i versus η for Solution Nos. 1 through 4 (Figure 3) shows that Solution Nos. 3 and 4 do in fact exhibit Tafel behavior above 50 mV and that the slope of the plots is about 59 mV/decade, which is consistent with the product of αn being 1.0. The plot for Solution No. 2 deviates slightly with a slope of 70 mV/decade while the plot for Solution No. 1 has a slope of 230 mV/decade in the Tafel region, which is a nonsequitur. Table 6 summarizes the steady-state data for the anodic reaction and includes the Tafel slope, values for the exchange current density (i_o) obtained by extrapolating the log i versus η data to zero overpotential, and the current density observed at 100 mV overpotential.

Although the plot of Solution No. 1 data does not exhibit reasonable Tafel behavior, an exchange current density can still be calculated with data obtained at low overpotentials. At small overpotentials, the Butler-Volmer equation can be approximated by Equation 7:

$$i = i_o \left(- \frac{nF\eta}{RT} \right) \tag{7}$$

This equation predicts that in the relatively narrow range of potentials near the equilibrium potential, the net current is linearly related to the over

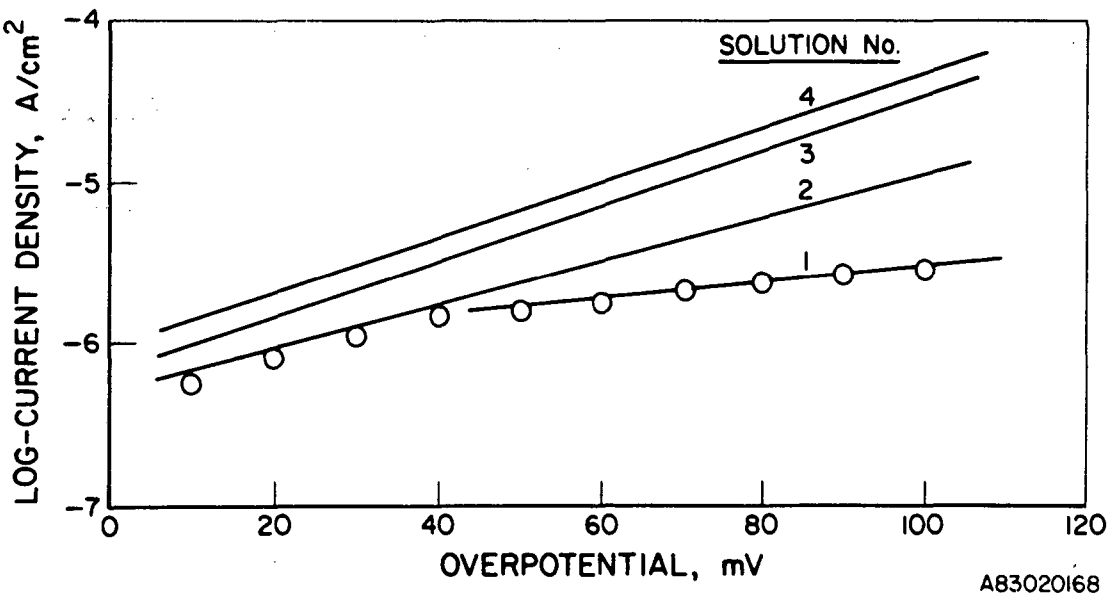


Figure 3. TAFEL PLOTS FOR ANODIC REACTION IN 1M SODIUM HYDROXIDE

Table 6. STEADY-STATE DATA FOR ANODIC REACTION*

Solution No.	Tafel Slope	Exchange Current Density, A/cm^2	Current Density at 100 mV Overpotential, A/cm^2
1	Linear plot**	3.2×10^{-7}	2.8×10^{-6}
2	73	5.0×10^{-7}	8.8×10^{-6}
3	60	6.6×10^{-7}	2.9×20^{-5}
4	58	8.9×10^{-7}	4.1×10^{-5}
12	56	5.0×10^{-7}	4.7×10^{-5}
13	67	1.0×10^{-6}	3.5×10^{-5}
14	65	1.6×10^{-6}	4.9×10^{-5}

* Obtained using a platinum wire electrode in a well stirred solution under nitrogen.

** Assumed n = 2.

potential. Thus an exchange current density (i_o) of 3.2×10^{-7} A/cm^2 is calculated for the anodic reaction of Solution No. 1 by ploting i versus η using data obtained near the equilibrium potential and by assuming n equals 2.

The data obtained from the steady-state investigation of the cathodic reaction are not well behaved. Current densities at 100 mV overpotential are about an order of magnitude less than those observed for the anodic reaction. Furthermore, the current-voltage data do not exhibit classical Tafel relationships, but deviate in a manner that suggests poisoning of the electrocatalyst. Figure 4 is a linear plot of i versus η for Solution Nos. 1 through 4. Although the data points for each solution fall on a line, comparison of data between solutions is confused. For example, we would expect the plot of i versus η for Solution No. 1 to be nearly flat because this solution contains only sulfide. (No zero-valent sulfur was detected in the UV-visible spectrum down to 100 ppm.) Indeed, the rest potential of a platinum electrode in this solution was 40 mV negative of the equilibrium potential measured in Solution No. 2. (See Table 1.) To sustain even small amounts of steady-state current, therefore, we would expect that the potential of the platinum cathode would have to be moved close to the equilibrium potential for the next most likely electrochemical reduction, Reaction 8:

$$2H_2O + 2e^- \rightarrow H_2 + 2OH^- \qquad (8)$$

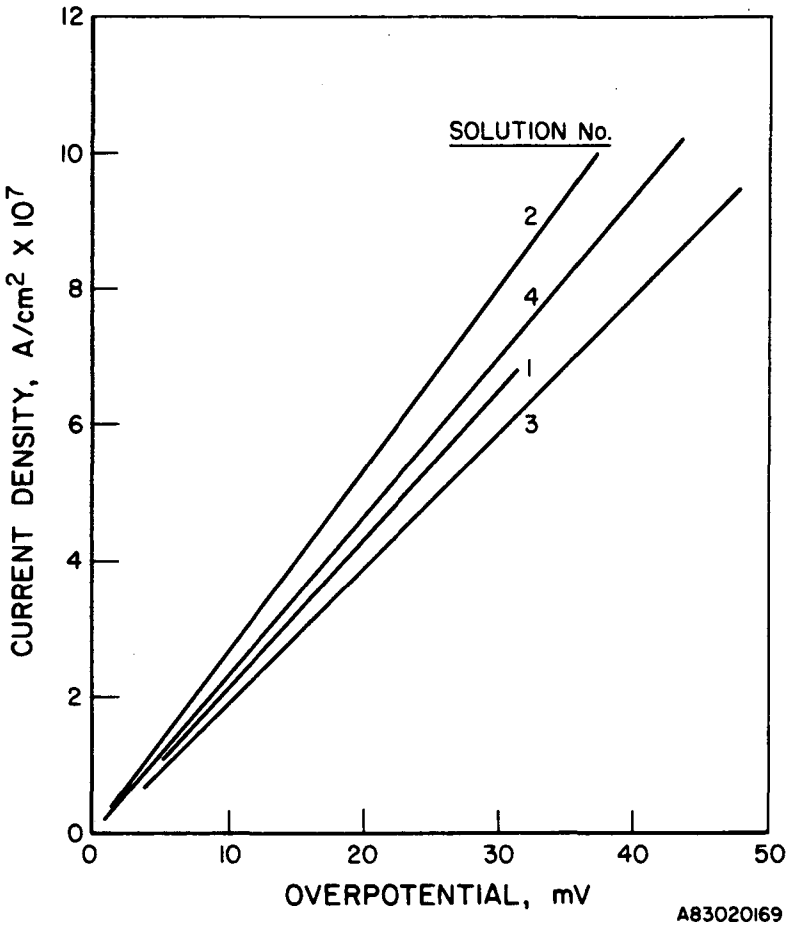


Figure 4. LINEAR PLOT OF CURRENT DENSITY VERSUS OVERPOTENTIAL FOR CATHODIC REACTION IN 1M SODIUM HYDROXIDE (Solution Nos. 1-4)

In 1.0M NaOH the equilibrium potential for Reaction 8 is near —1.06 V versus SCE, or about 300 mV negative of its measured rest potential. Instead, Solution No. 1 exhibited a steady-state current at 30 mV overpotential, which is higher than that observed for Solution No. 3 with 0.05M zero-valent sulfur. Such behavior could be explained by the presence of an as yet unidentified impurity. Two such possibilities are thiosulfate in the sodium sulfide nonahydrate (0.03 wt %) and carbonate in the sodium hydroxide (0.20 wt %). If this were the case, then all of the data reported in Figure 4 could be compromised by the presence of impurities.

Figure 5 is a linear plot of i versus η for the solutions using 1M sodium chloride as a supporting electrolyte. This figure shows the expected relationship between zero-valent sulfur and current density. That is, Solution No. 13 has 50% more zero-valent sulfur than Solution No. 12, and it exhibits a 50% higher current density at 10 mV overpotential. However,

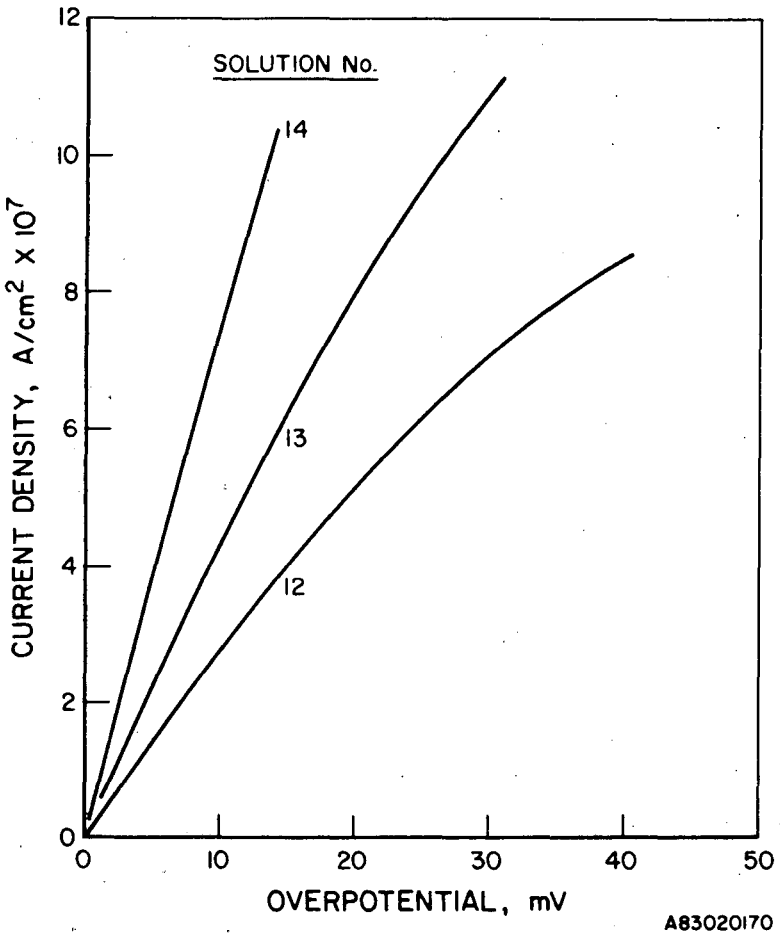


Figure 5. LINEAR PLOT OF CURRENT DENSITY VERSUS OVERPOTENTIAL FOR CATHODIC REACTION IN 1M SODIUM CHLORIDE (Solution Nos. 12-14)

careful examination of the lines for Solution Nos. 12 and 13 indicate that they curve at higher overpotentials in a direction that indicates an exponential increase in overpotenial with linear increases in current. This is contrary to the results expected for a typical linear plot. At high overpotentials, the current density should increase exponentially with linear increases in overpotenial (the Tafel relationship). Such a departure from the expected result indicates either mass transfer effects or catalyst poisoning.

Table 7 lists the exchange current densities for the cathode reaction, as determined on the basis of Equation 7, and for the current density observed at 100 mV overpotential.

Discussion

If we accept Equation 4 as describing the overall electrochemistry of the sulfide/polysulfide couple, we might expect the current density at 100 mV

Table 7. STEADY-STATE DATA FOR CATHODIC REACTION

Solution No.	Exchange Current Density,* A/cm^2	Current Density at η = 100 mV, A/cm^2
1	2.8×10^{-7}	1.3×10^{-6}
2	3.5×10^{-7}	2.2×10^{-6}
3	2.6×10^{-7}	2.5×10^{-6}
4	3.0×10^{-7}	3.0×10^{-6}
12	3.7×10^{-7}	2.6×10^{-6}
13	5.9×10^{-7}	3.3×10^{-6}
14	1.0×10^{-6}	4.4×10^{-6}

* Assumes that $\eta = 2$ in Equation 7.

overpotential, for the anodic reaction, to steadily decrease from Solution No. 1 to No. 4. This is based on steadily decreasing sulfide ion concentration. But the data in Table 6 show a marked increase in current density with decreasing sulfide concentration — the reverse of the expected trend. Allen and Hickling also reported this phenomenon and used it as a basis for postulating a reaction mechanism. Allen and Hickling supposed the initial step in the electrode reaction to be the adsorption of a polysulfide ion onto the metal surface:

$$S_x^{2-} + M \rightarrow M\text{---}S_x^{2-} \qquad (9)$$

The second step in the reaction is the interaction of this adsorbed polysulfide with a polysulfide ion in solution. In this step two electrons are transferred from the adsorbed polysulfide to the metal electrode, and the outermost sulfur atom of the adsorbed polysulfide adds to the terminal atom of the polysulfide in solution:

$$M\text{---}S_x^{2-} + S_x^{2-} \rightarrow M\text{---}S_{x-1} + S_{x+1}^{2-} + 2e^- \qquad (10)$$

This leaves a zero-valent sulfur species adsorbed on the metal surface. The reaction is complete, and the surface is regenerated by addition of a sulfide ion from solution:

$$M\text{---}S_{x-1} + S^{2-} \rightarrow M\text{---}S_x^{2-} \qquad (11)$$

Of course, this final step must be adjusted to account for the hydrogen we now know accompanies the sulfide in solution:

$$M\text{---}S_{x-1} + HS^- + OH^- \rightarrow M\text{---}S_x^{2-} + H_2O \qquad (12)$$

Allen and Hickling proposed that the electron transfer step (Equation 10) is the rate-determining step.

Two key points in this mechanism are the requirements for polysulfides in solution and for an active catalyst layer of adsorbed polysulfides. The anomalous behavior exhibited by Solution No. 1 (Figure 3) can now be explained by the lack of polysulfides in solution to carry on the rate-determining step.

The ability of polysulfides but not sulfide ions to strip zero-valent sulfur from the catalyst surface can be explained, at least in part, by partial charge distribution. Meyer et al.[8] calculated the charge distribution for the sulfane family using an extended Huckel model. They determined the portion of the negative (2-) charge on each atom of the polysulfide chain for the whole polysulfide family up to S_8. Their results indicate that for S_3^{2-}, the two terminal atoms each carry a partial negative charge of —0.70, and the central sulfur atom carries —0.60 of the total —2.0 charge. For S_4^{2-} each terminal atom has a partial charge of —0.59, and each of the two interior atoms carries —0.41 of the total —2.0 charge. The charge on the terminal atoms for each of the remaining members of the polysulfide series is as follows: —0.52 for S_5^{2-}, —0.50 for S_6^{2-}, —0.48 for S_7^{2-}, and —0.47 for S_8^{2-}. The charge on the first members of this series, of course, do not require calculation. Sulfide would have a charge of —2.0, and disulfide (S_2^{2-}) would have a charge of —1.0 on each atom. Although the charge distribution between the hydrogen and the sulfur atoms in HS^- was not treated in the Meyer et al. paper, the partial charge on the sulfur should be between —0.8 and —1.0. The charge distribution on the terminal atom becomes important when we consider that charged ions in aqueous solution are surrounded by a hydration sphere of water molecules. The higher the charge on the ion, the more tightly held will be the hydration sphere. If we postulate that in the rate determining step (Equation 10) the neutral sulfur atom on the surface of the catalyst adds to the terminal atom of the polysulfide chain, then the hydration sphere must be perturbed. We would expect the larger polysulfides with loosely held hydration spheres to be most facile in this reaction. If, on the other hand, we postulate that the neutral sulfur adds across two interior atoms of the poly-

sulfide, the argument still holds because the partial charge residing on the interior atoms of the polysulfide also decreases with chain length. Thus, on the basis of the Allen and Hickling mechanism, we would expect the current density for the anodic reaction to increase with increasing zero-valent sulfur content.

We can now take this one step further. In light of Giggenbach's work discussed above, as the pH of the solution decreased we would expect zero-valent sulfur to be found in fewer but longer polysulfide species. Thus, although Solutions Nos. 2 and 12 were initially formulated with the same sulfide-to-sulfur ratio, Giggenbach's work predicts that Solution No. 12 would contain fewer but longer polysulfide ions than Solution No. 2. The same can be said for Solution Nos. 3 and 13 and for Nos. 4 and 14. Table 6 indicates that at constant overpotential higher current densities are observed with Solution Nos. 12, 13, and 14 than with their respective counterparts Nos. 2, 3 and 4. This is strong evidence that the partial charge on the terminal sulfur atoms affects the rate of reaction to a greater extent than differences in concentration. Thus, the Allen and Hickling mechanism, the work of Giggenbach, and the work of Meyer et al. can be used in concert to explain all the phenomenon observed here for the anodic reaction.

When this was applied to the cathodic reaction, however, we quickly come to the following conclusions: Either the Allen and Hickling mechanism does not work in reverse and Reaction 4 is in fact irreversible, or the catalytic surface required is either not present initially or is destroyed when voltages negative of the equilibrium potential are applied. Fortunately, the cyclic voltammetric investigation shed considerable light on the problem.

Cyclic Voltammetry

Results

For every solution investigated, cyclic voltammograms were recorded using a smooth platinum wire electrode with a geometrical surface area of 0.85 cm^2. Two separate voltammograms were recorded for each solution. The platinum electrode was prepared by wiping it with a soft, clean, lint-free cloth of a type commonly used to clean optical equipment. The electrode was then rinsed with "spectro" grade acetone, air dried, and placed in the solution under investigation 0.05-cm away from a Luggin capillary attached to

a SCE. After sparging the solution with nitrogen for 30 minutes, a cyclic voltammogram was recorded starting at the equilibrium potential and scanning first in the negative direction to within 60 mV of the reversible hydrogen potential and then in the positive direction to within about 60 mV of the oxygen potential. Potential cycling was continued between these two points at a sweep rate of 100 mV/s. The first three complete cycles were recorded on a single graph; the recorder was then disengaged, loaded with new graph paper, and the 20th cycle was also recorded. Figure 6 is representative of the kind of information obtained on the 20th cycle. This particular voltammogram is for the 20th cycle of a smooth platinum wire in Solution No. 2 (0.067M sulfide + 0.033M sulfur + 1.0M hydroxide). The following three observations are important in Figure 6:

1. The peak anodic current is considerably larger than the peak cathodic current
2. The peak anodic and cathodic currents are separated by over 500 mV
3. The equilibrium potential (—0.72 V) does not represent a point of zero current flow on the 20th voltammogram, but rather the zero current point is over 150 mV positive of the equilibrium potential.

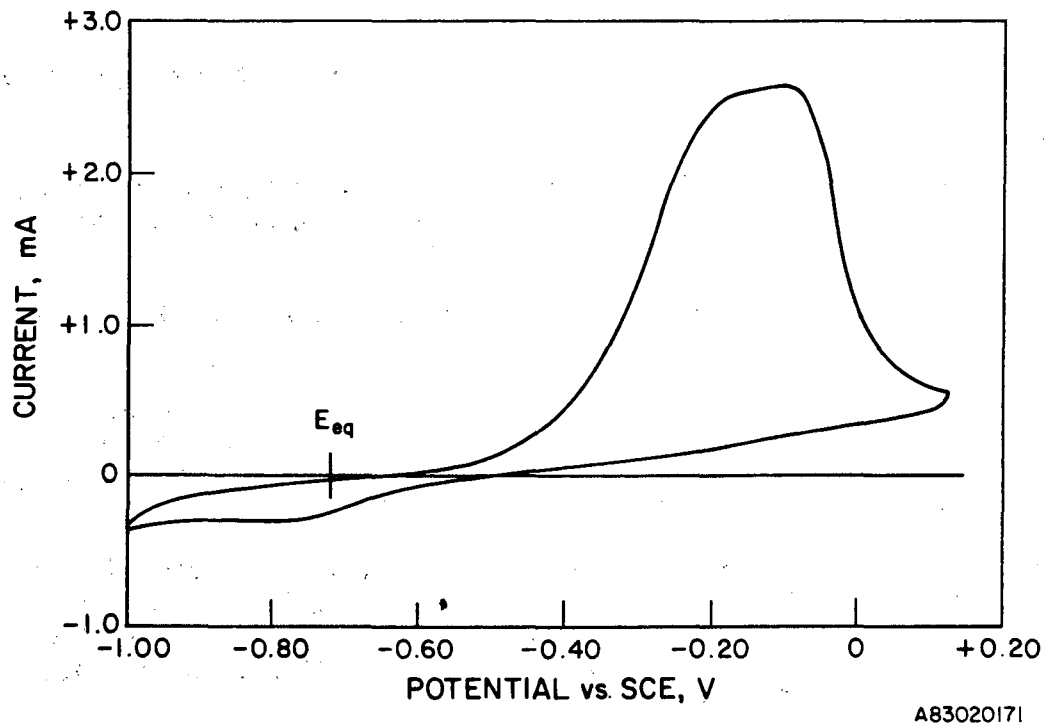


Figure 6. CYCLIC VOLTAMMOGRAM FOR THE 20TH CYCLE USING A 0.85 cm^2 PLATINUM WIRE ELECTRODE IN SOLUTION No. 2 (Scan Rate: 100 mV/s)

Although some minor differences were noted, 20th cycle voltammograms of all solutions tested exhibited the above three anomalies.

Figure 7 represents the cyclic voltammogram for the first three cycles of a platinum wire electrode in Solution No. 2. The cycle was started at the equilibrium potential and proceeded first in the negative direction at a rate of 100 mV/s. The potential was cycled in a continuous linear sweep between a negative limit of —1.00 V and a positive limit of +0.10 V as measured versus a SCE. The first scan of the cathodic reaction is labeled 1C, and the first anodic scan is labeled 1A. The following points are of significance in Figure 7:

1. No current is observed on the first cathodic scan (1C).

2. The first anodic scan, 1A, exhibits a minor anodic ware at -0.50 V, which is not present in subsequent anodic scans.

3. The second cathodic scan, 2C, shows a substantial cathodic current with a maximum of about 1.3 mA/cm^2

4. All cycles subsequent to the first cycle exhibit a cathodic current at E_{eq} regardless of the direction of the voltage sweep.

5. Both the peak anodic and cathodic currents diminish with cycle number, collapsing ultimately to Figure 6.

Other important observations made during this and other voltammetric experiments are as follows:

1. The minor anodic wave at —0.50 V in Figure 7 was present in all first-cycle voltammograms in the same relative position with respect to E_{eq} regardless of the supporting electrolyte used.

2. The minor anodic wave was present on the first cycle regardless of whether the cycle began with a negative or a positive voltage sweep.

3. Placing the cell on open circuit for 10 seconds did not regenerate this minor anodic wave. However, maintaining the open circuit for 10 minutes with rapid electrolyte stirring did regenerate the minor anodic wave to its full intensity in the subsequent first-cycle scan.

4. If the potential limits of the cyclic voltammogram were reduced to —1.00 to —0.20 V versus SCE (a reduction in the positive limit only), no decrease in the maximum anodic and cathodic currents was observed with repeated cycling. In other words, the cyclic voltammogram for Cycle 2 was identical to that for Cycle 20.

5. Careful examination of the wire electrode after continuous cycling between —1.00 and +0.10 V indicated a layer of sulfur had built up on the electrode. However, this sulfur layer was not present when the positive potential limit was reduced to —0.20 V.

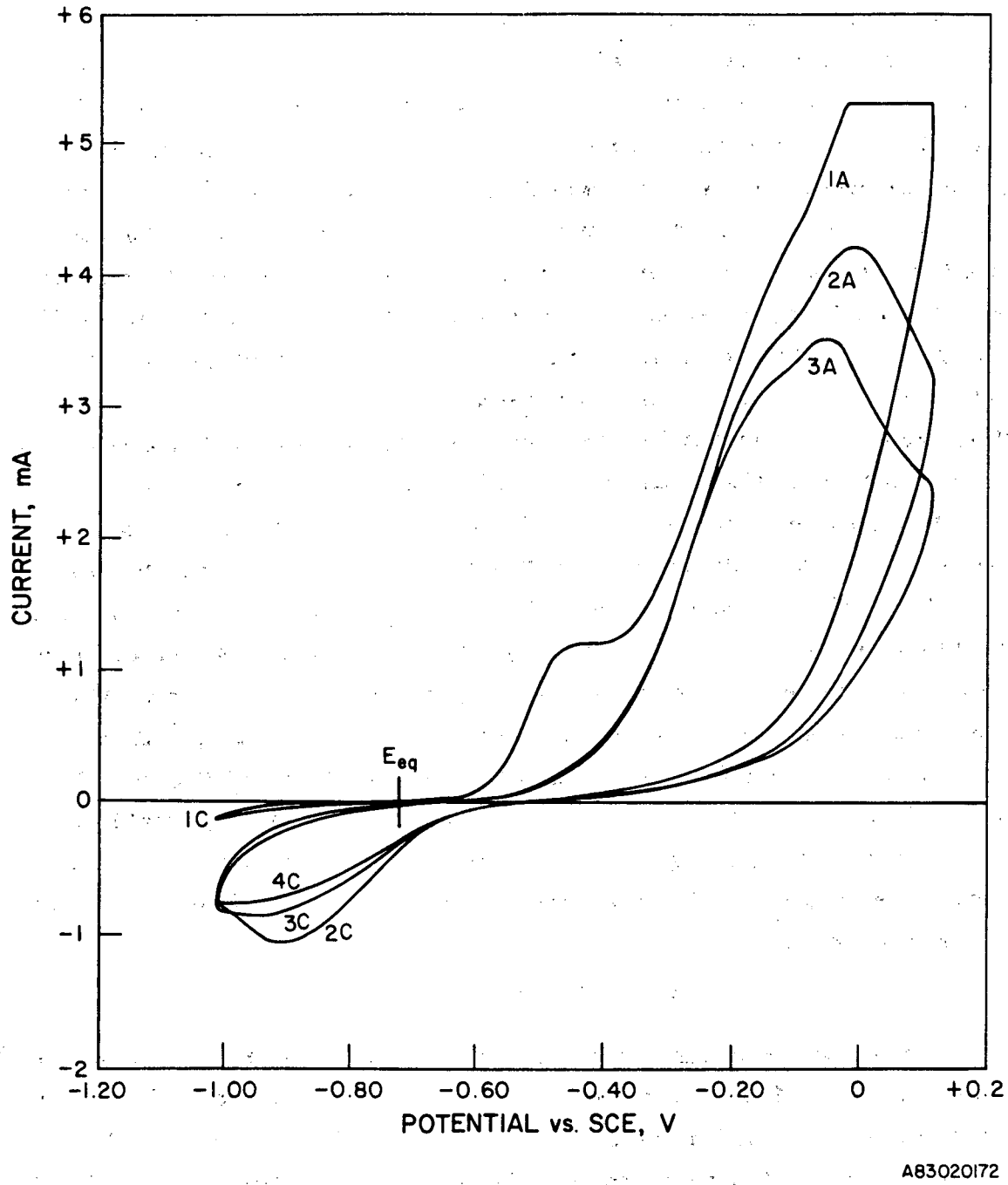


Figure 7. CYCLIC VOLTAMMOGRAM FOR THE FIRST, SECOND, AND THIRD CYCLES USING A PLATINUM WIRE IN SOLUTION No. 2 (Scan Rate: 100 mV/s)

Discussion

Figure 7 shows that the cathodic reaction does not work on a clean platinum electrode. Scan 1C shows virtually no current flow through the first 100 mV of negative potential displacement from E_{eq} — a result that parallels those obtained in the steady-state study. Subsequent cathodic scans did exhibit substantial cathodic currents, but only after the electrode was subjected to potentials several hundred millivolts positive of E_{eq}. This argues in favor of one of the tentative conclusions drawn in the discussion of the steady-state results: The catalytic surface required for the reaction is not present initially on smooth platinum electrodes. More importantly, the small anodic wave observed only on the first cycle could represent the electrochemical formation of such a catalytic layer. The first step in the reaction mechanism proposed by Allen and Hickling was the adsorption of a polysulfide onto the electrode surface, (Equation 9). There is no reason to believe that such an adsorption would be spontaneous on platinum, or that the adsorption of polysulfide would be preferred over the adsorption of sulfide. In fact, the lack of a cathodic current in Scan 1C argues against the inner Helmholtz plane even containing any polysulfide. On the other hand, we might postulate that there are specifically adsorped sulfide ions in the IHP. Although inactive during negative potential deviations from E_{eq}, these adsorped sulfide ions are oxidized at potentials positive of E_{eq} to form a layer of adsorbed sulfur atoms much in the same manner that hydroxide ions form a layer of adsorbed oxygen atoms on platinum at potentials near the reversible oxygen potential. This reaction (13) is responsible for the small anodic wave at —0.50 V:

$$Pt---S^{2-} \rightarrow Pt---S + 2e^{-} \qquad (13)$$

We can further postulate that these adsorbed sulfur atoms act as sites for the attachment of polysulfide as required in the first step of the Allen and Hickling mechanism. Such an absorbed sulfur atom would be expected to be inherently unstable at potentials negative of —0.50 V. However, the presence of the attached polysulfide may either stabilize the adsorbed sulfur or protect it sterically such that the cathodic reaction observed in 2C, 3C, etc., is the reduction of polysulfide rather than the destruction of the catalytic layer.

RESULTS AND DISCUSSION OF TASK 2

Assessment of Electrocatalytic Activity

Task 1 work had two important results: 1) platinum is an exceedingly poor electrocatalyst for the reduction of polysulfide, and 2) a surface-adsorbed sulfur species is required in the proposed reaction mechanism. This suggests that electronically conducting metal sulfides such as NiS, CoS, and MoS_2 might make excellent electrocatalysts for both anodic and cathodic reactions. To test this hypothesis, micropolarization measurements were made using wire electrodes of these three metals and their sulfides suspended in solution. Solution No. 13, with a concentration of 0.05M Na_2S, 0.05M sulfur, and 1.0M NaCl, was chosen because its sulfide/polysulfide ratio is most representative of a partially discharged redox battery. We should emphasize, however, that an actual redox flow battery using the sulfide/polysulfide couple would use concentrations in the range of 1M to 2M total sulfur.

Metal sulfide wire electrodes were prepared from elemental stock by sulfidation in an H_2S atmosphere. In the case of nickel and cobalt, sulfidation was performed in a tube furnace at 400°C by heating the wire to temperature in an argon atmosphere and then switching to a 50% Ar/50% H_2S mixture for 1 hour. The sample was then cooled under this gas mixture. A similar procedure was used for molybdenum sulfide, but at 500°C. Microscopic examination of the sulfided nickel indicated a substantial increase in surface roughness. Gold-colored crystallites of nickel sulfide now populated the surface of what had been a relatively smooth nickel wire. Cobalt exhibited a slight increase in surface roughness, although it was not as pronounced as with the nickel. Sulfided molybdenum, however, exhibited a gun-metal blue color that upon microscopic examination showed no change in surface luster or roughness when compared to the stock molybdenum wire. Exchange current densities were calculated from measured currents at various potentials near the equilibrium potential using Equation 7. Table 8 lists the results. Results for molybdenum metal have not been included because subsequent experiments indicated significant anodic corrosion of the unprotected metal at potentials positive of the equilibrium potential. Blue molybdenum sulfide (MoS_2), on the other hand, is quite stable in alkaline and alkaline sulfide solutions.

Table 8. EQUILIBRIUM POTENTIAL AND EXCHANGE CURRENT DENSITY FOR VARIOUS METALS AND THEIR SULFIDE IN SOLUTION NO. 13

Electrode	E_{eq} vs SCE, V	I_o,* A/cm^2
Co	−0.651	5.0×10^{-6}
CoS	−0.630	9.4×10^{-6}
Ni	−0.645	3.3×10^{-6}
NiS	−0.650	9.5×10^{-6}
Pt	−0.644	1.0×10^{-6}
MoS_2	−0.638	3.0×10^{-6}

* Based upon geometrical surface area.

Significantly, Table 8 shows that 1) the equilibrium potentials agree with one another to within ±3%; and 2) although the exchange current density for the metal sulfides is slightly higher than for the corresponding metals, they are all of the same order of magnitude.

The significance of the first observation is that the measured equilibrium potential is the rest potential of the sulfide/polysulfide couple and not a corrosion potential, as represented by Equation 14:

$$x\ S^{2-} + M \rightleftarrows MS_x + 2xe^- \qquad (14)$$

The significance of the second observation is that if the Allen-Hickling mechanism is correct, and an adsorbed sulfide or other sulfur species is the active site, then the similar exchange current densities for the various metal sulfides indicate that the metals that accompany the sulfides exert similar electrocatalytic influence.

Nickel Sulfide (NiS)

Latimer lists the standard reduction potential for the alpha-form of nickel sulfide as −0.83 V. If the sulfide ion activity in Solution No. 13 is assumed to be equal to the sulfide ion concentration (0.05M), the reversible electrode potential for Equation 15 is −1.034 V versus SCE:

$$S^{2-} + Ni \rightleftharpoons NiS + 2e^- \qquad (15)$$

Because the equilibrium potential for the sulfide/polysulfide couple in this solution is only —0.65 V versus SCE, we would expect nickel sulfide to be stable. Figure 8 is a cyclic voltammogram of a sulfided nickel wire in Solution No. 13. A reduction wave at about —1.0 V versus SCE exhibits an increase in cathodic current upon reversal of the scan direction. Such a phenomenon may indicate an increase in surface area as a result of sulfide loss via dissolution.

Figure 8 suggests that nickel sulfide has acceptable stability in the potential range from —0.850 to —0.40 V versus SCE in Solution No. 13. But we would expect the reduction potential for nickel sulfide (Equation 15) to show about half of the sulfide ion dependence as the equilibrium potential for the sulfide/polysulfide couple (Equation 4). At higher concentrations of sulfide, therefore, the cathodic limit of the stability region would move closer to the sulfide/polysulfide equilibrium potential. Thus, if nickel sulfide were used as an electrocatalyst in a practical device where concentrations of 1M to 2M sulfide would be expected, cathodic overpotentials would have to be limited to less than 150 mV to avoid reduction of the electrocatalyst.

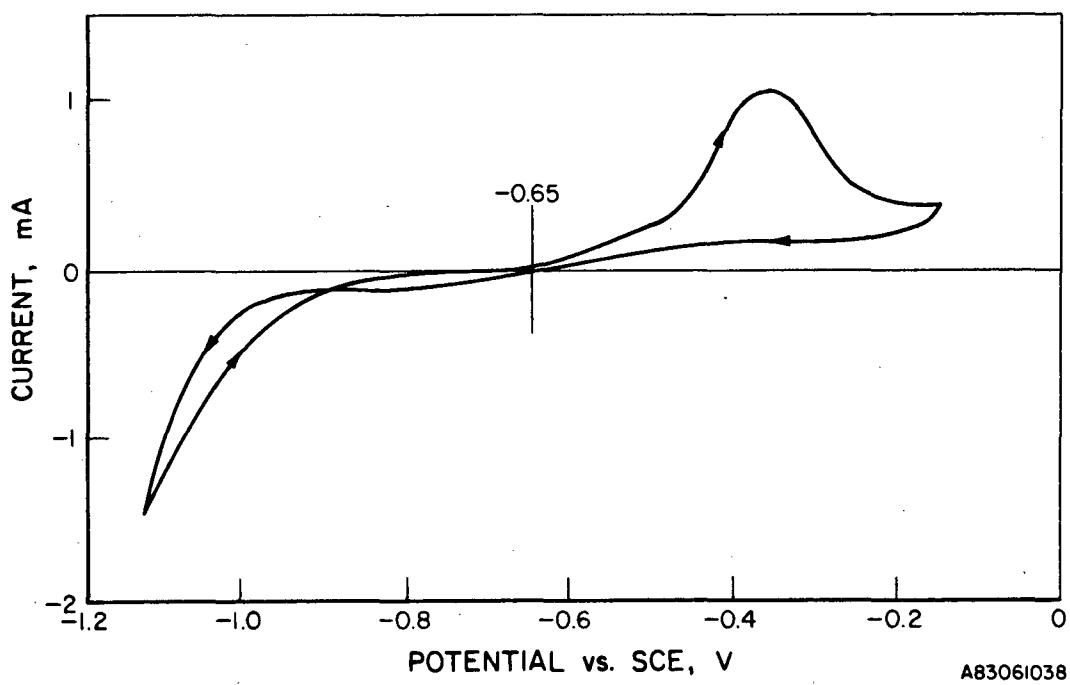


Figure 8. CYCLIC VOLTAMMOGRAM OF NICKEL SULFIDE IN SOLUTION No. 13 (Surface Area, 0.22 cm^2; Scan Rate 10 mV/s)

Cobalt Sulfide (CoS)

Latimer places the standard reduction potential for the alpha-form of cobalt sulfide at —0.90 V, which is about 70 mV more negative than nickel or about —1.10 V versus SCE in Solution No. 13. Yet the cyclic voltammogram for cobalt sulfide in this solution (Figure 9) differs markedly from that of nickel sulfide. In contrast to nickel sulfide, the anodic portion of the voltammogram for cobalt sulfide is well behaved and does not exhibit electrode passivation — nor does the cathodic portion indicate radical changes in surface area. The cyclic voltammogram for cobalt sulfide exhibits two cathodic waves: a small wave at about —0.95 V versus SCE and a larger wave whose shape suggests a passivating process centered at about —1.10 V versus SCE. Note that the reversible hydrogen potential in Solution No. 13 is about —0.98 V versus SCE. Therefore, the slight decrease in performance observed at —0.95 V on the cathodic scan may be the result of poisoning of the catalytic surface by adsorbed hydrogen. We have no clear evidence to support

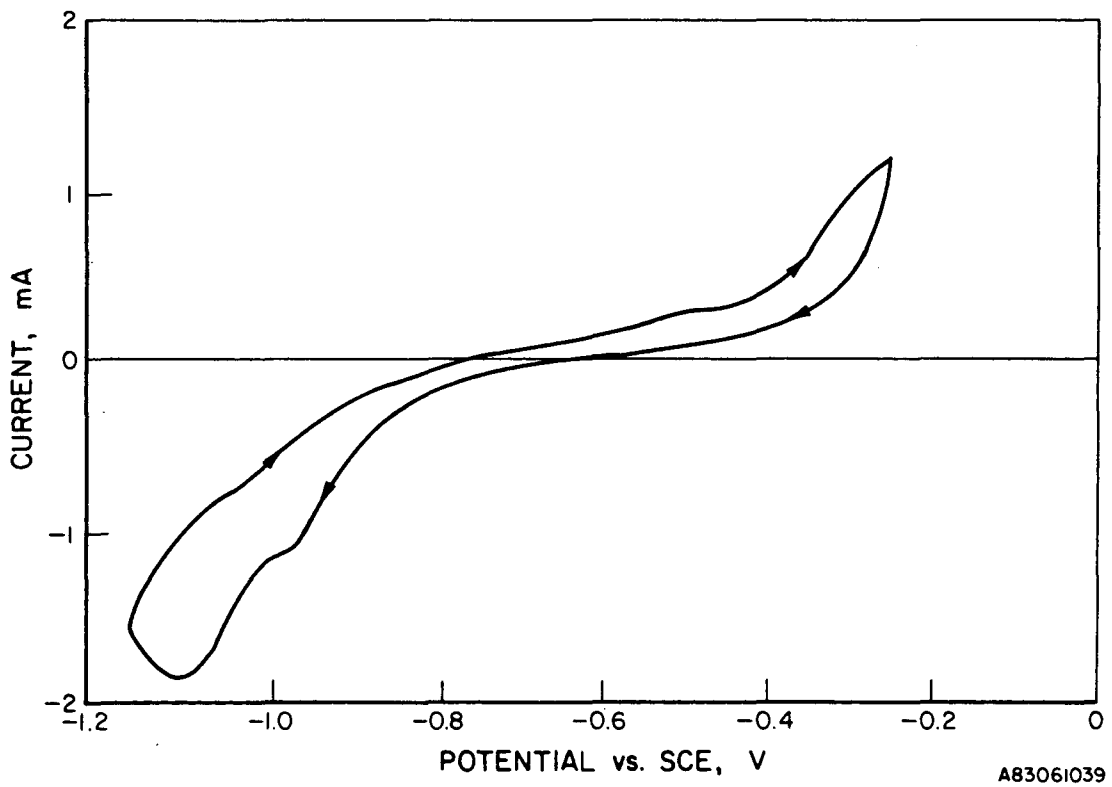


Figure 9. CYCLIC VOLTAMMOGRAM OF COBALT SULFIDE IN SOLUTION No. 13 (Surface Area, 0.50 cm^2; Scan Rate, 10mV/s)

this, however. Clearly, the cyclic voltammogram shows that cobalt sulfide is a useful electrocatalyst for the sulfide/polysulfide couple and has a range of stability extending from —0.950 to —0.300 V versus SCE.

Molybdenum Sulfide (MoS_2)

Although there are a number of molybdenum sulfides ranging in composition from the sesquisulfide (Mo_2S_3) to the tetrasulfide (MoS_4), the most stable molybdenum sulfide is the disulfide, which is insoluble in alkaline sulfide solutions and is formed upon heating molybdenum metal in an H_2S atmosphere. Little information regarding the electrochemistry of MoS_2 exists in the literature so it is not possible to estimate a reversible potential for its electrochemical reduction under our conditions. As a consequence of this lack of information, some preliminary experiments were conducted with pure molybdenum metal.

When molybdenum metal was placed in Solution No. 13 it assumed a potential of —0.724 V versus SCE. This behavior contrasts markedly with that of nickel and cobalt metals, which like platinum assumed the potential of the redox couple (about —0.65 V versus SCE). The cyclic voltammogram of molybdenum metal in this solution (Figure 10) shows a high corrosion current at —0.4 V versus SCE. The shape of the voltammogram and subsequent microscopic examination of the electrode suggested that a soluble corrosion product is formed. Note that the pentasulfide, trisulfide, and tetrasulfide of molybdenum ($Mo_2S_5 \cdot 3H_2O$, MoS_3, and MoS_4, respectively) are all soluble in alkaline sulfide solution. Another anomaly observed in this voltammogram is the indication of an anodic current at potentials positive of —1.0 V versus SCE but well negative of the equilibrium potential of the redox couple. This anodic current is observed only during the portion of the cycle when the potential is moving in the positive direction. One possible explanation for the shape of this cyclic voltammogram is the formation of an insoluble sulfide such as Mo_2S_3 at potentials positive of —1.0 V versus SCE followed by further oxidation to a soluble species such as Mo_2S_5 at potentials positive of —0.4 V.

Experiments conducted with a sulfided molybdenum electrode produced by heating a molybdenum wire to 500°C in hydrogen sulfide gave no evidence of corrosion in Solution No. 13. Figure 11 is a cyclic voltammogram of this molybdenum sulfide electrode under the same conditions of sulfide/polysulfide

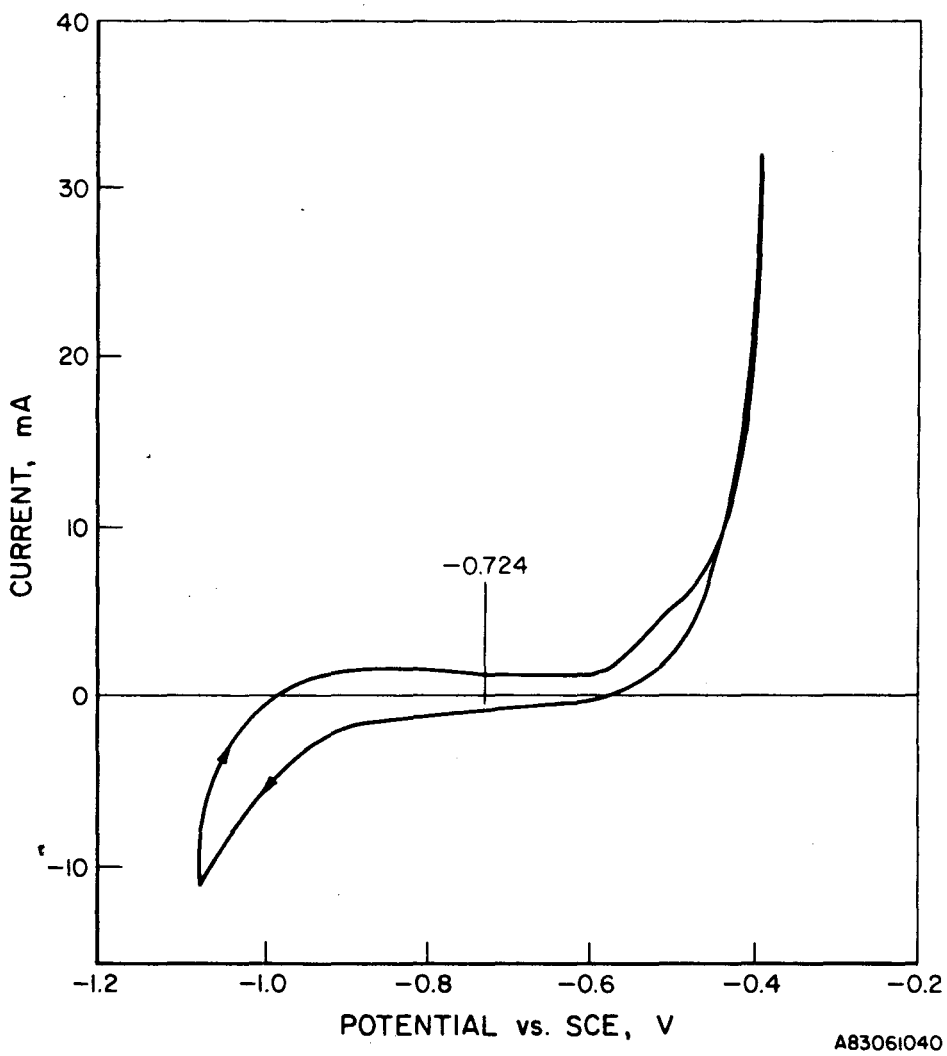


Figure 10. CYCLIC VOLTAMMOGRAM OF MOLYBDENUM WIRE IN SOLUTION No. 13 (Surface Area, 2.90 cm^2; Scan Rate, 100 mV/s)

concentration, pH, and scan rate as was used with the molybdenum wire in Figure 10. Noticeably absent is the corrosion current at —0.45 V and evidence of an anodic current at potentials between —0.9 and —0.7 V. Data accumulated over several weeks indicate that this electrode is very stable in sulfide solutions over the potential range from —1.0 to —0.4 V versus SCE.

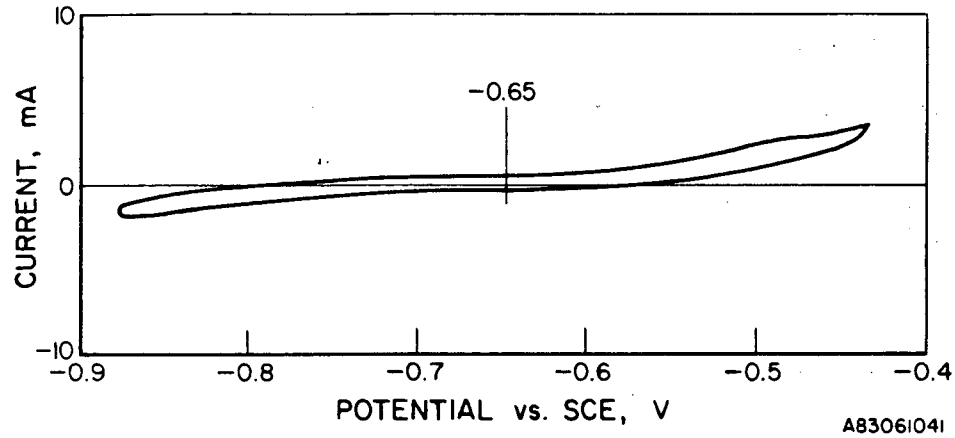


Figure 11. CYCLIC VOLTAMMOGRAM OF MOLYBDENUM WIRE WITH MOLYBDENUM COATING IN SOLUTION No. 13 (Surface Area, 2.4 cm^2; Scan Rate, 100 mV/s

Concentration Effects on Electrode Performance

A sulfided molybdenum wire electrode was chosen for this investigation because of its relatively smooth surface. Examination of a sulfided molybdenum wire using optical microscopy indicated that no change in surface roughness or luster occurred during the sulfidation process, although the color was altered from grey metallic (Mo) to blue metallic (MoS_2). This contrasts with sulfidation of cobalt and nickel where scales were formed that created problems in reproducibility. The MoS_2 coated electrode was placed in a test solution of a specific concentration and connected to a potentiostat. Beginning with the equilibrium potential (point of zero current) E_{eq}, the electrode potential was scanned in steps: first to a potential 100 mV negative of E_{eq}, then to a potential 100 mV positive of E_{eq}, and then back again. The rate of change in potential was 1.5 mV/min in 1 mV steps. This approach was taken to produce a plot of current density versus overpotential data under steady-state conditions. It was reasoned that in a practical redox device the electrodes would seldom operate outside this range of polarizations to assure cycle efficiency. Four solutions were chosen for this test, all

Table 9. PARAMETERS INVESTIGATED AND RESULTS OBTAINED FOR THE POLARIZATION OF MoS_2 WIRE ELECTRODES IN SOLUTIONS OF VARYING CONCENTRATION

Solution Number	3	13	130	1302
Total Sulfur, M	0.10	0.10	1.0	2.0
Supporting Electrolyte	NaOH	NaCl	NaCl	None
E_{eq}-measured vs. SCE	-0.710	-0.635	-0.716	-0.761
E_{eq}-calculated from Equation 6	-0.706	-0.640	-0.721	-0.745
Exchange Current Density from Equation 7	2.8×10^{-6}	2.8×10^{-6}	1.4×10^{-5}	2.5×10^{-5}

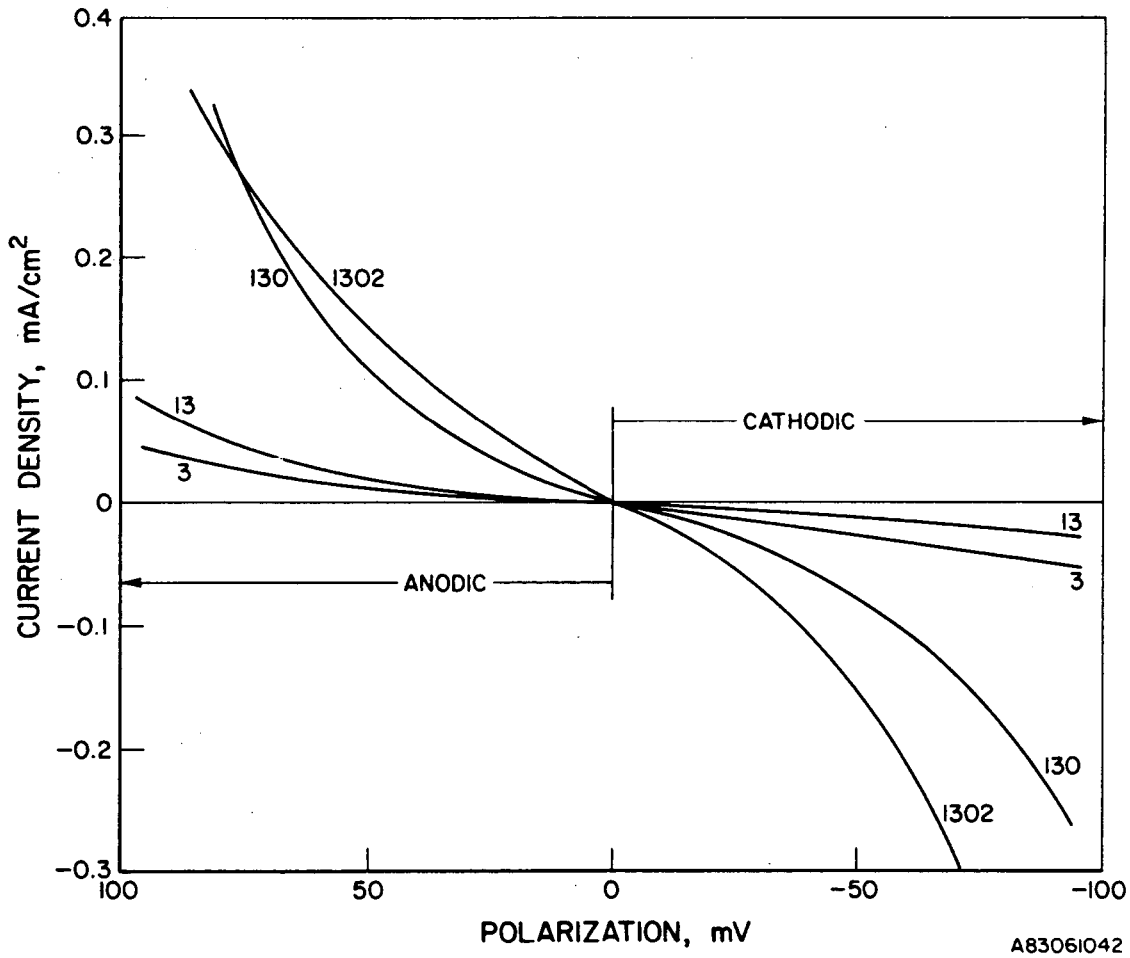


Figure 12. PERFORMANCE OF MoS_2 WIRE ELECTRODE IN SOLUTIONS OF VARYING CONCENTRATION

with the same 1:1 ratio of sodium sulfide to elemental sulfur, but differing in total sulfur concentration and in supporting electrolyte composition. The results of these experiments are plotted as current versus overpotential in Figure 12. Numerical results of particular interest are summarized in Table 9.

The results in Figure 12 are as expected, with two exceptions. First, the performance of the molybdenum sulfide electrode appears to be better in Solution No. 13 than in Solution No. 3 for the anodic reaction, but is worse for the cathodic reaction. Second, at higher anodic polarizations, the current density is less with the solution containing 2M total sulfur than with the solution containing 1M total sulfur. At the present time we have no explanation for either of these anomalies.

Composite Electrodes

Because both molybdenum sulfide and cobalt sulfide are expensive materials, we decided to direct the final efforts in this project toward the fabrication of inexpensive composite electrodes. In pursuit of this goal an 80% carbon, 10% molybdenum sulfide, 10% Teflon composite electrode was fabricated. The carbon used as a support was Vulcan XC-72R supplied by the Cabot Corporation of Boston, Massachusetts. This material is an electrically conducting carbon black of about 250 m^2/g surface area with a mean particle size of 30 nm. The molybdenum sulfide was obtained from Cerac, Inc., of Milwaukee, Wisconsin, and was a 99% pure powder with an average particle size of 1 micron. Teflon 30 was chosen as a binder. The fabrication procedure is as follows.

One hundred milligrams of molybdenum sulfide was mixed with 800 mg of carbon black. A water dispersion of Teflon 30 was then added in sufficient quantity to provide approximately 10 wt % of Teflon solids in the final dried composite. These materials were mixed thoroughly, and the wet composite, which was the consistency of putty, was spread uniformly onto a nickel screen using firm pressure on a hand-held spatula.

The electrode was dried at 95°C for 30 minutes, and the composite was firmly pressed a second time with the spatula. The electrode was then heated in an oven at 330°C for 15 minutes to drive off all dispersing agents and to sinter the Teflon fibers. The electrode was then removed and pressed between

two nickel foil platens heated to approximately 250°C. Pressing time was about 3 minutes at 500 lb on the 1/4-in.^{2} (1.4 cm^2) electrode.

This composite electrode was placed in Solution No. 130 and cycled in steps as described above. Figure 13 is a plot of the data for this electrode. Current densities, based upon geometrical surface area, are nearly an order of magnitude higher with this composite electrode than with a smooth molybdenum sulfide electrode. This increase in performance can most assuredly be attributed to the high surface area of the supported catalyst. Repeated cycling of this electrode over 3 days indicated no loss in activity.

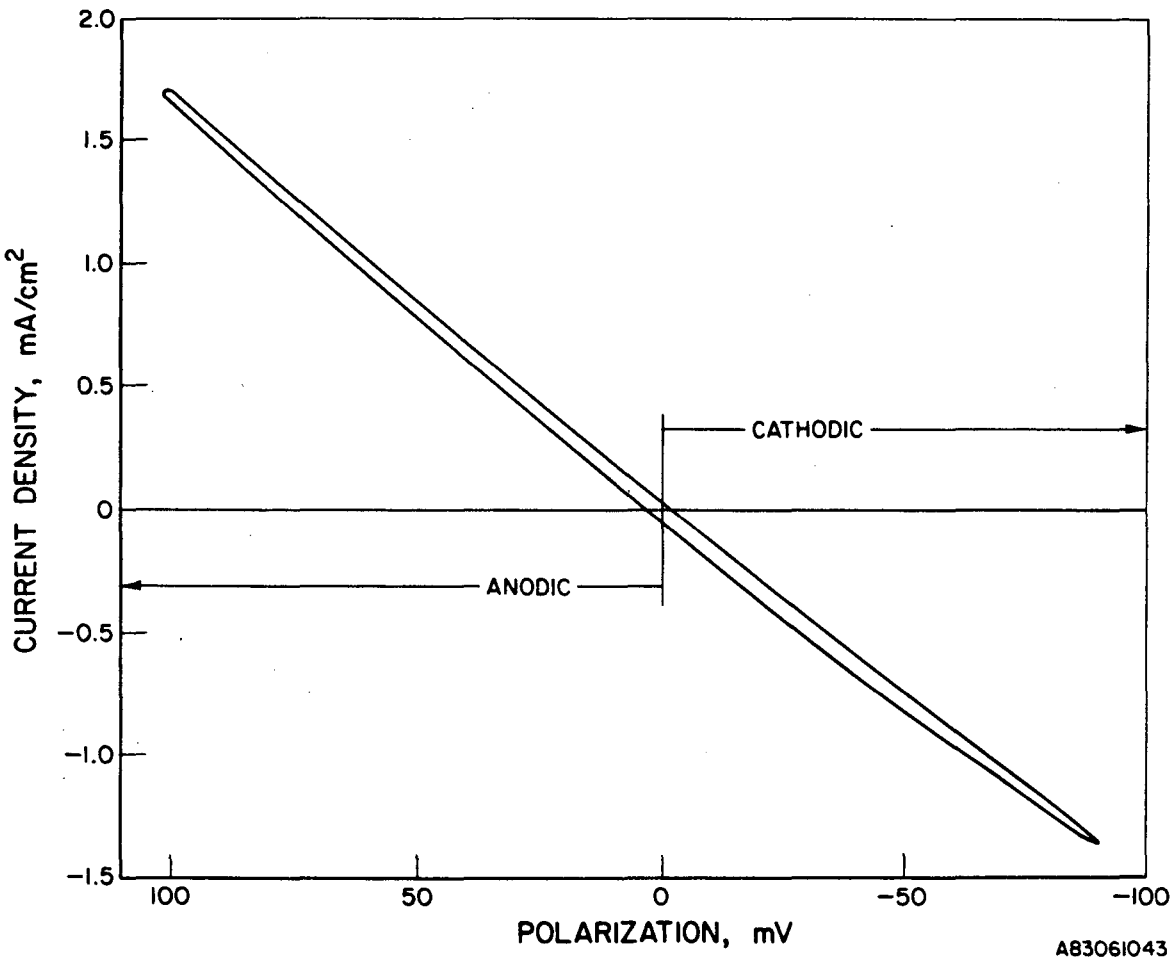


Figure 13. PERFORMANCE OF COMPOSITE ELECTRODE IN SOLUTION No. 130

CONCLUSIONS

We have confirmed that the mechanism originally proposed by Allen and Hickling in 1957 to describe the redox behavior of sulfides and polysulfides in aqueous solution is essentially correct. The mechanism presupposes the existence of a catalytic layer of sulfur species on the electrode surface. Experimental results presented here suggest that the poor performance of platinum electrodes for the cathodic reduction of polysulfide is the result of the absence or loss of this catalytic layer. We have also confirmed that electronically conducting metal sulfides are good electrocatalysts for both sulfide oxidation and polysulfide reduction. Experiments conducted on solid metal wires sulfided in an H_2S atmosphere, however, indicate that exchange current densities for the anodic reaction are, at best, only a few times higher than found on smooth platinum. This fact, together with the Allen and Hickling mechanism, strongly supports the catalytic sulfide layer hypothesis, because in every case the surface sulfur species is active rather than the metal. As a consequence, little difference in exchange current density is found between metal sulfides. On the other hand, metal sulfides such as CoS and MoS_2 are stable toward cathodic reduction in the range of potentials necessary for polysulfide reduction. Therefore, they are greatly superior to platinum as electrocatalyts for the cathodic reaction.

We have also demonstrated that inexpensive composite electrodes can be fabricated using small amounts of supported metal sulfide catalysts.

REFERENCES CITED

1. Allen, P. L. and Hickling, A., "Electrochemistry of Sulfur," Trans. Faraday Soc. 53, 1626 (1957).

2. Giggenbach, W., "Optical Spectra of Highly Alkaline Sulfide Solutions and the Second Dissociation Constant of Hydrogen Sulfide," Inorg. Chem. 10 1333 (1971).

3. Giggenbach, W., "Optical Spectra and Equilibrium Distribution of Polysulfide Ions in Aqueous Solution at 20°," Inorg. Chem. 11, 1201 (1972).

4. Hodes, G., Manassen, J. and Cahen, D., "Electrocatalytic Electrodes for the Polysulfide Redox System," J. Electrochem. Soc. 127, 544 (1980).

5. Hodes, G., Manassen, J. and Cahen, D., "Effect of Surface Etching and Morphology on the Stability of CdSe/S_x^{2-} Photoelectrochemical Cells," J. Electrochem. Soc. 128, 2325 (1981)

6. Ives, D. J. G., "Oxide, Oxygen, and Sulfide Electrodes," in Reference Electrodes: Theory and Practice, Chapter 7, p 379. New York: Academic Press, 1961.

7. Meyer, B., Sulfur, Energy, and Environment. New York: Elsevier, 1977.

8. Meyer, B., Peter, L. and Spitzer, K., "Trends in the Charge Distribution in Sulfanes, Sulfanesulfonic Acid, Sulfanedisulfonic Acid, and Sulfurous Acid," Inorg. Chem. 16, 27 (1977.

9. Noufi, R. N. et al., "An Investigation of S/Se Substitution in Single Crystal CdSe and CdS Photoelectrodes by Elecron Spectroscopy," J. Electrochem. Soc. 126, 949 (1979).

10. Remick, R. J., Ang, P. G. P. and Sammells, A. F., "On the Feasibility of Sulfur-Iodine Redox Storage Batteries." Paper presented at the October 5-10 Meeting of the Electrochemical Society, Hollywood, Fla. 1980 Abstract No. 151.

4H/RPE/LBL

This report was done with support from the Department of Energy. Any conclusions or opinions expressed in this report represent solely those of the author(s) and not necessarily those of The Regents of the University of California, the Lawrence Berkeley Laboratory or the Department of Energy.

Reference to a company or product name does not imply approval or recommendation of the product by the University of California or the U.S. Department of Energy to the exclusion of others that may be suitable.

TECHNICAL INFORMATION DEPARTMENT
LAWRENCE BERKELEY LABORATORY
UNIVERSITY OF CALIFORNIA
BERKELEY, CALIFORNIA 94720